Mechanical Behavior of Flax-Lime Concrete Blocks made of Waste Flax Shives and Lime Binder Reinforced with Jute Fabric

Krishna Priyanka Garikapati and Pedram Sadeghian[1]

Department of Civil and Resource Engineering, Dalhousie University, 1360 Barrington Street, Halifax, NS, B3H 4R2, Canada.

Abstract:

Due to the increase in production of construction materials, the emission of carbon dioxide levels and the requirement for producing materials with a less environmental footprint is gaining more attention. This paper focuses on the study of a special kind of concrete (without stone aggregates) called flax-lime concrete to decrease amount of environmental footprint via the use of a lime-based binder with a waste material of flax fiber production (i.e. flax shives). Nine flax-lime concrete beam specimens (51 mm x 152 mm x 610 mm) with the same mix proportions were prepared. A layer of jute fabric mesh was also placed at the center of the specimens as a reinforcement. The position and number of layers of the fabric mesh were varied to improve the load capacity and deflection under three-point bending. The physical and mechanical properties (namely: density, load-carrying capacity, failure mode, and load-deflection behavior) of the flax-lime concrete specimens were studied. Overall, the variation in position and number of layers of jute fabric increased the bending capacity and energy absorption in flax-lime concrete blocks. The system can be used in buildings for infilling masonry blocks and filling wall cavities as insulation materials.

Keywords: flax; shive; waste; lime; recycling.

https://doi.org/10.1016/j.jobe.2020.101187

[1] Assistant Professor and Canada Research Chair in Sustainable Infrastructure. Email: Pedram.Sadeghian@dal.ca (corresponding author)

1. INTRODUCTION

The process of manufacturing concrete raw materials and other building materials require large amount of energy for production. High levels of greenhouse gases, especially carbon dioxide (CO_2), are produced in the process. One idea is replacing some of the construction materials with plant-based materials to reduce CO_2 levels. Base on the need, new concepts in construction materials that offer co-benefits of energy efficiency and thermal comfort is likely to gain momentum in the building industry [1]. New concepts based on bio-based materials such as straw bale constructions [2], date palm fibers [3], and corrugated cardboard [4] for building applications are emerging. Plant-based materials help to absorb CO_2 as they grow and can replace non-renewable fibers such as glass fibers [5][6][7][8]. Natural fibers such as flax, hemp, jute, etc. can be used as reinforcement for construction materials [9][10][11][12]. The production of natural fibers from stalk of their plants typically results in short woody by-products known as shives or hurds [13][14][15][16]. Hemp shives have been mixed with a lime-based binder in the form hemp-lime concrete also known as hempcrete [17][18][19][20][21].

Numerous studies have been conducted on hemp-lime concrete. For example, Ip and Miller [22] investigated the levels of emission of greenhouse gases from hemp-lime concrete wall, throughout its life cycle. The mix proportions of binder used for hemp-lime concrete wall, 75% of hydrated lime ($Ca(OH)_2$), 15% of hydraulic lime (CaO), and 10% of pozzolans. The amount of CO_2 emission was obtained 36.08 kg per wall from the time of construction till the end of the life span of the wall with the volume of 0.3 m^3.

Nguyen et al. [13] studied hemp-lime made of a binder, containing 75% non-hydraulic lime of total volume of binder, 15% hydraulic lime, and 10% pozzolan. The ratio of binder to hemp was changed from 2.12 to 2.77 (for low compaction) whereas water to binder ratio was kept constant at

0.5. It was concluded that the hemp-lime concrete had a high deformation capacity prior to compression failure when heavy compaction was applied. Whereas, at low compaction, hemp lime concrete had low resistance to compression.

Barnat-Hunek et al. [23] investigated the mechanical and thermal properties of hemp-lime concrete. Six batches of hemp-lime concrete were prepared, and several tests were conducted to see how properties were being varied with different mix proportions. Three cubic specimens (100 mm dimension) were prepared from each batch to test bulk density and absorptivity. It was concluded that if the amount of hemp shives increased, absorptivity decreased, and bulk density increased. In addition, there was reduction in the compressive strength with increase in hemp percentage.

There have been several experiments [24][25][26][27][28] conducted on the thermal conductivity of hemp-lime concrete. Overall, hemp-lime concrete has been studied since the 2000's with a focus on the characterization of its hygrothermal properties and prediction of the temperature and humidity inside the material and in the surrounding air [29][30]. Generally, hemp-lime concrete is highly porous with open and interconnected porosity. It has been shown that thermal conductivity is varied by the moisture content and density of hemp lime concrete.

As described, majority of research work has been done on hemp shives. In this study, hemp-lime concrete studies were taken as reference to choose proportion of materials to be used in flax-lime concrete. The aim of this paper is to study how flax shives mixed with a lime-based binder work as a construction material, especially targeting insulation blocks to be placed in wall cavities in building with stud and drywall system and infilled masonry frames. The system can be also cast-in-place for the wall cavities.

2. MATERIALS AND METHOD

In this section an experimental program is described on the use of flax-lime concrete for building applications. First, the constituent materials of flax-lime concrete is explained followed by test matrix, specimen preparation, and tests set-up.

2.1. Materials

For the production of flax-lime concrete, flax shives (with the length less than 25 mm) were obtained from a local farm in Nova Scotia, Canada. The average bulk density of flax shives in a cylindrical container (100 mm diameter and 200 mm height) casted in three layers and compacted with a 10 mm diameter tamping rod (25 stroke per layer) was obtained 141 kg/m^3. Fast binder, an autoclaved lime (92% hydrated) and general use (GU) Portland cement were mixed in proportion of 4:1 by volume, respectively. Flax shives, binder, and tap water were mixed in proportion of 4:1:1 by volume, respectively, to prepare the flax-lime concrete mixture. An all-purpose burlap (jute fabric mesh) was used to reinforce the test specimens. The openings of the jute fabric mesh were approximately 5 mm x 5mm providing an integration between flax-lime concrete and the reinforcement.

2.2. Test Matrix

As shown in Table 1, nine beam specimens were prepared out of flax-lime concrete for testing with a rectangular cross-section of 152 mm x 51 mm and length of 610 mm. A jute fabric mesh was used at mid-height for control specimens and at a quarter-height from bottom for remaining specimens to act as a reinforcement (Figure 1). One layer of jute fabric (610 mm x 152 mm) was placed in six specimens and two layers jute fabric was placed in remaining specimens to study how number of jute fabric layers effect strength of the specimen. The beam specimens are identified as Lx-yH, where x indicates the number of jute fabric layers and y indicates the location ratio of the jute fabric from the

bottom of the specimen. For example, specimen L2-0.25H contains two layers of jute fabric at quarter of the height from the bottom of the specimen. In addition to the beam specimens, three cylindrical specimens (100 mm diameter and 200 mm height) were prepared to evaluate the compressive behavior of flax-lime concrete materials.

2.3. Specimen Preparation

Initially, a wooden formwork was prepared to cast the specimens as shown in Figure 2. Grease was applied to the formwork. To prepare the binder, 4 parts of lime and 1 part of cement (by volume) were well mixed until a uniform mixture was obtained. Then, 4 parts flax shives were taken into a bowl and 1 part of the binder were added to it. Flax shives and binder were mixed thoroughly by hand until a uniform mixture was obtained. Then, 1 part of water was added and again it was mixed thoroughly by hand. All the mixture was transferred into the formwork and compacted in four layers using one stroke per square inch per layer using a square tamping rod with 25 mm x 25 mm cross-section. For L1-0.5H specimens, when formwork was filled to half of the height, one layer of the jute fabric mesh was placed and then the next two layers of flax-lime were cast and compacted as explained until the formwork was filled. All four layers were similarly compacted by the tamping rod and strokes were given along the whole layer in the same pattern. Then, the specimen was covered with a plastic cover and transferred to curing room. For L1-0.25H and L2-0.25H specimens, when formwork was filled to the quarter of the height, one and two layers of the jute fabric mesh was placed, respectively, and then the next three layers of flax-lime were cast and compacted. For the compression tests, three cylindrical plastic molds (100 mm diameter and 200 mm height) were filled with 8 layers of flax-lime concrete and compacted with one stroke per square inch per layer using the square tamping rod. Then, all the specimens with formwork were placed in a curing room for 7 days and then transferred to the lab to be dried at room temperature. After at least 28 days of casting, the beam specimens were

weighed, and volumes were measured. The weights and volumes were used to calculate the bulk density of each specimen. The average bulk density of all nine beam specimens was obtained 559 kg/m^3 with a standard deviation of 49 kg/m^3. Then, the specimens were tested per the following section.

2.4. Test Setup and Instrumentation

For testing the beam specimens, a hydraulic loading frame was initially planned to be used for testing the specimens, however the frame's load cell was not sensitive enough to capture the capacity of the specimens. As a result, a manual three-point bending loading setup was prepared and weights were gradually placed at the center of test the specimen as shown in Figure 3. Two roller supports, two displacement dial gauges, and multiple weights were used for testing the specimens. The span between rollers was maintained at 559 mm. A small plate was also placed on a specimen to hold the dial gauges. Once everything was set, known weights were placed at the center of the specimen, and the dial gauges were read. The weights were gradually added to the specimen and enough intervals between each weight was maintained to ensure the dial gauges were stabilized. Figure 4 shows photos of one of the specimens before and during loading. The procedure was continued up the failure of the specimen. The load at each step was calculated based on the weights and mid-span deflection was obtained from the average of two dial gauges. The compression cylinders were tested using a hydraulic self-reaction frame. Two digital displacement gauges were recorded the total axial deformation of each cylinder and a load cell provided the load during the test until failure.

3. RESULTS AND DISCUSSION

In this section, the test results are presented, and a discussion is provided on failure modes, load deflection behavior, and energy absorption of the test specimens.

3.1. Failure Modes

Figure 5 shows typical failure modes of the beam specimens. Overall, as the load increased, a flexure crack was initiated from the bottom of the specimen and was gradually propagated to the top by producing a cracking sound. The width of crack was also observed to be increased on addition of weights. The jute fabric showed its effect on the gradual crack propagation of the specimens. It was observed that the visible portion of the crack can only propagate up to the location of the jute fabric. Consequently, the region above the jute fabric remained without any visual damage. For the specimens with the jute fabric at the quarter of the height from the bottom, the crack width was smaller than those with the jute fabric located at mid-height. With increasing the number of jute fabrics to two layers, the failure was more gradual showing a ductile behavior. Overall, moving the location of the jute fabric from mid-height to the bottom quarter-height increase the load bearing capacity of the flax-lime beams. The overall failure the beam specimen can be characterized with a large bending deformation due to yielding flax-lime in compression.

3.2. Compressive Behavior

In order to evaluate the compressive behavior of flax-lime concrete, three cylinders were prepared and tested under pure axial compression load as shown in Figure 6. Each cylinder was placed between two steel plate and the top plate was moved down by a hydraulic jack. Two string potentiometers were used to measure the relative movement of the plates. The axial displacement of the cylinder was obtained by averaging the data from the string potentiometers and divided by the height of the cylinder to calculate axial stroke strain. A load cell was used to obtain the load and divided by the cross-section of the cylinder to calculate axial compressive stress. The stress-strain curves are presented in Figure 7. As seen, the curves are similar to the curve obtained by applying load on foam materials [31]. All

the three stages of foam curve (i.e. linear elasticity, yielding, and densification [32]) are visible in Figure 7. Similar behavior was previously observed for hemp-lime concrete [18][33]. Based on Figure 7, the yielding strength of the flax-lime concrete is about 200 kPa, which is comparable with that of low-density foams for sandwich panels [34]. A summary of compression test results is presented in Table 2.

3.3. Load-Deflection Behavior

Figure 6 shows the load vs. the mid-span displacement of all nine beam specimens. The mid-span displacement of each specimen was obtained by averaging the displacement from two parallel dial gauges. Each group of curves are related to a set of specimens (namely L1-0.5H, L1-0.25H, and L2-0.25H) with three identical specimens. As shown in the figure, the load-deflection behavior of the specimen is non-linear with a short initial linear region before any cracking. With forming the first tension crack at the bottom face, the load deflection become nonlinear. As the cracks propagate upward, the behavior become more non-linear. When the crack reaches to the location of the jute fabric, the crack stabilizes, and the jute reinforcement is activated to resist the bending moment. As presented in Figure 5, the specimens with jute fabric at mid-height (i.e. L1-0.5H) was not able to resist the load similar to the rest of specimens as the jute fabric was not activated early enough. Thus, the strain at the compression region exceeded the linear strain of flax-lime in compression and the material in the compression region entered the plastic region with large deformation ended up to an overall failure of the beam specimens.

The three specimens with one layer of jute fabric at H/4 position from bottom (i.e. L1-0.25H) showed significant increase in load and average displacement that is 2 times compared to L1-0.5H specimens. Whereas specimens with 2 layers of jute fabric at H/4 (i.e. L2-0.25H) did not show much difference in load as compared to L1-0.25H specimens. However, there was prominent increase in

average displacement, which indicates number of layers does not influence the load capacity but increase in number of jute fabric layers help to increase average displacement. This can be related to low compressive strength of flax-lime concrete and entering the extreme compressive layer of the beams into the yielding region as shown in Figure 7. By yielding flax-lime in compression, the jute fabric's tensile force was capped, and the beams were not able to support more loads than shown in Figure 8. As a result, the load-deflection behavior of the specimens entered a plateau region with a shallow slope. In this region, flax-lime was in yielding region with a slight gain in strength (see Figure 7) and the jute fabric was able to support the additional load until the rupture/stretch of the jute fibers. The specimens with two layers of jute fabric were able to sustain more plastic deflection as two layers of fabric provided more strength than one layer of fabric. Ultimately, the rupturing/stretching of the jute fabric caused large deformations and test was terminated.

It should be highlighted that the standard deviation of yielding and failure loads for beam L1-0.25H is significantly higher than other two beams (see Table 3). This might be related to the fact that placing the jute fabric mesh at 0.25H from the bottom created significant amount of tensile stress in the fabric. As the fabric was thin with large mesh size, this possibly created stress concentration on jute fibers with low volume fraction. By adding another layer of the jute fabric, corresponding volume fraction was doubled reaching a point that rupturing a few fibers under high stress concentration did not affected the overall strength of the fabric due to redistribution of stress to other fibers. Certainty, providing enough fiber volume fraction needs to be considered for practical designs securing required safety margin.

3.4. Idealized Bending Behavior

The bending behavior of the specimens can be idealized as a tri-linear behavior as shown in Figure 9. Point A is cracking of flax-lime in tension at the extreme tension face, point B is yielding of flax-lime

in compression at the extreme compression face, and Point C is the ultimate point corresponding to rupture/stretch of jute fabric. In region AB, the behavior of flax-lime specimen is linear without any damage. After cracking (Point A), the specimen is cracked, and jute fabric is activated. As the section is cracked, the stiffness is lower that initial region. By reaching the flax-lime to yielding the extreme compression face (Point B), the stiffness decreases significantly, and the curve continues in region BC with a shallow slope compatible with the shallow slope of flax-lime in compression after yielding. By reaching to Point C, the jute fabric ruptures/stretches causing large deformations which can be considered the ultimate capacity of the system.

Based on Figure 8, the cracking load of the specimens is approximately about 30 N, which is translated into the tensile strength of about 64 kPa, which is about 30% of the compressive yielding strength of 200 kPa obtained from the cylinder tests. Table 3 shows the summary of the test results based on yielding and failure points of B and C. The maximum average loads at Point B and C were obtained as 260 N and 285 N, respectively, for L1-0.25H specimens. The maximum average displacements at Point B and C were obtained at 8.2 mm and 21.1 mm, respectively for L2-0.25H specimens. There was significant increase in displacement when two layers of jute fabric were used in L2-0.25H specimens, which was about 2 times the L1-0.25H specimens and 5 times the L1-0.5H specimens. The load capacity at yielding Point B increased twice when the position of jute fabric was changed from 0.5H to 0.25H in L1-0.25H specimens.

3.5. Energy Absorption

Energy absorbed by each specimen was calculated using the area under the curve of a specimen and the results are shown in Table 3. It can be observed that L2-0.25H specimens (Set 3) absorbed energy almost two times of L1-0.25H specimens (Set 2) and almost 14 times of L1-0.5H specimens (Set 1).

3.6. Future Studies

Advanced nonlinear modeling is needed to predict the yielding and ultimate points. It should be noted that strain compatibility in the specimens is applicable as long as there is bond between the jute fabric mesh and flax-lime concrete. After yielding since flax-lime concrete was producing wider cracks strain compatibility may not be applicable. Further research concerning the strain distribution across the specimen depth is needed. Also, the thermal conductivity of the material and blocks needs to be studied in depth.

4. POTENTIAL APPLICATIONS

The proposed flax-lime concrete reinforced with jute fabric can be used for infilling masonry blocks in building frames and insulation applications. The flax-lime concrete blocks can be designed to have the right dimensions filling the cavity building walls with stud and drywall system. Insulation of walls not only makes a significant difference in the comfort of a home, but it is also essential for reducing energy costs. Also, flax-lime concrete can be placed in the cavity walls using cast-in-place methods. This method is labor and time intensive, however can provide a better air seal than blocks. However, the flax-lime concrete blocks can be manufactured and cured in a factory with a controlled density and insulation properties. As flax-lime is relatively light-weight in comparison with other concrete/cementitious-based products, the blocks can be transported to construction sites and placed in cavity walls much easier than cast-in-place products. The blocks may need to be reinforced using the proposed jute fabric mesh based on their dimension to support their self-weight during transportation and keep their integrity for installation. More in-depth study is needed in this area to propose the system for the building insulation applications.

5. CONCLUSIONS

In this paper, several specimens made of flax-lime concrete reinforced with a jute fabric mesh were prepared and tested under bending. After at least 28 days of casting, the average density of the specimens was obtained as 559 kg/m^3. Flax-lime concrete showed a compressive behavior similar to insulation foam materials with yielding and densification regions. Base on the tests, yielding compressive strength of 200 kPa and tensile rupture strength of 64 kPa was obtained for the flax-lime concrete studied in this paper. The bending behavior of the specimens was idealized as a tri-linear behavior with three distinctive points namely, cracking of flax-lime in tension, yielding and flax-lime in compression, and failure of the beams by rupture/stretching of jute fabric. The crack started from the bottom of the specimen and propagated to the height where jute fabric was placed. Whereas the failure crack was not observed above the jute fabric showing the effectiveness of the fabric in crack control. From the point of yielding to failure, the specimens did not take much load due to yielding behavior of flax-lime in compression, however increasing number of jute fabric increased the ductility of the beam specimens. Potential application as infilling and insulation blocks for building applications were identified. In the future, flax-lime concrete need to be investigated in depth on mechanical and thermal conductivity properties before using as a construction material.

6. ACKNOWLEDGEMENTS

The authors acknowledge the contribution of TapRoot Fibre (Port Williams, NS, Canada) for providing flax shives. Also, Dr. Fadi Oudah of Dalhousie University is thanked for his feedback on the draft research paper prepared by the first author.

7. REFERENCES

[1] Latha PK, Darshana Y, Venugopal V. Role of building material in thermal comfort in tropical climates–A review. Journal of Building Engineering. 2015 Sep 1;3:104-13.

[2] D'alessandro F, Bianchi F, Baldinelli G, Rotili A, Schiavoni S. Straw bale constructions: Laboratory, in field and numerical assessment of energy and environmental performance. Journal of Building Engineering. 2017 May 1;11:56-68.

[3] Belakroum R, Gherfi A, Bouchema K, Gharbi A, Kerboua Y, Kadja M, Maalouf C, Mai TH, El Wakil N, Lachi M. Hygric buffer and acoustic absorption of new building insulation materials based on date palm fibers. Journal of Building Engineering. 2017 Jul 1;12:132-9.

[4] McCracken A, Sadeghian P. Corrugated cardboard core sandwich beams with bio-based flax fiber composite skins. Journal of Building Engineering. 2018 Nov 1;20:114-22.

[5] Joshi, S.V., Drzal, L.T., Mohanty, A.K. and Arora, S., 2004. Are natural fiber composites environmentally superior to glass fiber reinforced composites?. Composites Part A: Applied science and manufacturing, 35(3), pp.371-376.

[6] Mishra, S., Mohanty, A.K., Drzal, L.T., Misra, M., Parija, S., Nayak, S.K. and Tripathy, S.S., 2003. Studies on mechanical performance of biofibre/glass reinforced polyester hybrid composites. Composites Science and Technology, 63(10), pp.1377-1385.

[7] Wambua, P., Ivens, J. and Verpoest, I., 2003. Natural fibres: can they replace glass in fibre reinforced plastics?. Composites science and technology, 63(9), pp.1259-1264.

[8] Hristozov, D., Wroblewski, L. and Sadeghian, P., 2016. Long-term tensile properties of natural fibre-reinforced polymer composites: comparison of flax and glass fibres. Composites Part B: Engineering, 95, pp.82-95.

[9] Yan, L., Chouw, N. and Jayaraman, K., 2014. Flax fibre and its composites–A review. Composites Part B: Engineering, 56, pp.296-317.

[10] Ku, H., Wang, H., Pattarachaiyakoop, N. and Trada, M., 2011. A review on the tensile properties of natural fiber reinforced polymer composites. Composites Part B: Engineering, 42(4), pp.856-873.

[11] Shahzad, A., 2012. Hemp fiber and its composites–a review. Journal of Composite Materials, 46(8), pp.973-986.

[12] Sadeghian, P., Hristozov, D. and Wroblewski, L., 2018. Experimental and analytical behavior of sandwich composite beams: Comparison of natural and synthetic materials. Journal of Sandwich Structures & Materials, 20(3), pp.287-307.

[13] Nguyen, T.T., Picandet, V., Amziane, S. and Baley, C., 2009. Influence of compactness and hemp hurd characteristics on the mechanical properties of lime and hemp concrete. European Journal of Environmental and Civil Engineering, 13(9), pp.1039-1050.

[14] Stevulova, N., Kidalova, L., Cigasova, J., Junak, J., Sicakova, A. and Terpakova, E., 2013. Lightweight composites containing hemp hurds. Procedia Engineering, 65, pp.69-74.

[15] Kymäläinen, H.R. and Sjöberg, A.M., 2008. Flax and hemp fibres as raw materials for thermal insulations. Building and environment, 43(7), pp.1261-1269.

[16] Elfordy, S., Lucas, F., Tancret, F., Scudeller, Y. and Goudet, L., 2008. Mechanical and thermal properties of lime and hemp concrete ("hempcrete") manufactured by a projection process. Construction and Building Materials, 22(10), pp.2116-2123.

[17] Shea, A., Lawrence, M. and Walker, P., 2012. Hygrothermal performance of an experimental hemp–lime building. Construction and Building Materials, 36, pp.270-275.

[18] Walker, R., Pavia, S. and Mitchell, R., 2014. Mechanical properties and durability of hemp-lime concretes. Construction and Building Materials, 61, pp.340-348.

[19] Elfordy, S., Lucas, F., Tancret, F., Scudeller, Y. and Goudet, L., 2008. Mechanical and thermal properties of lime and hemp concrete ("hempcrete") manufactured by a projection process. Construction and Building Materials, 22(10), pp.2116-2123.

[20] de Bruijn, P.B., Jeppsson, K.H., Sandin, K. and Nilsson, C., 2009. Mechanical properties of lime–hemp concrete containing shives and fibres. Biosystems engineering, 103(4), pp.474-479.

[21] Nguyen, T.T., Picandet, V., Carre, P., Lecompte, T., Amziane, S. and Baley, C., 2010. Effect of compaction on mechanical and thermal properties of hemp concrete. European Journal of Environmental and Civil Engineering, 14(5), pp.545-560.

[22] Ip, K. and Miller, A., 2012. Life cycle greenhouse gas emissions of hemp–lime wall constructions in the UK. Resources, Conservation and Recycling, 69, pp.1-9.

[23] Barnat-Hunek, D., Smarzewski, P. and Fic, S., 2015. Mechanical and thermal properties of hemp-lime composites. Composites Theory and Practice, 15(1), pp.21-27.

[24] Amziane S, Arnaud L. 2013. Bio-aggregate-based Building Materials: Applications to Hemp Concretes. John Wiley & Sons, Inc., Hoboken, New Jersey, USA.

[25] Benfratello, S., Capitano, C., Peri, G., Rizzo, G., Scaccianoce, G. and Sorrentino, G., 2013. Thermal and structural properties of a hemp–lime biocomposite. Construction and Building Materials, 48, pp.745-754.

[26] Collet, F. and Pretot, S., 2014. Experimental highlight of hygrothermal phenomena in hemp concrete wall. Building and environment, 82, pp.459-466.

[27] Kinnane, O., Reilly, A., Grimes, J., Pavia, S. and Walker, R., 2016. Acoustic absorption of hemp-lime construction. Construction and building materials, 122, pp.674-682.

[28] Walker, R. and Pavía, S., 2014. Moisture transfer and thermal properties of hemp–lime concretes. Construction and Building Materials, 64, pp.270-276.

[29] Seng B, Magniont C, Lorente S. Characterization of a precast hemp concrete. Part I: Physical and thermal properties. Journal of Building Engineering. 2019 Jul 1;24:100540.

[30] Seng B, Magniont C, Lorente S. Characterization of a precast hemp concrete block. Part II: Hygric properties. Journal of Building Engineering. 2019 Jul 1;24:100579.

[31] Fam, A., Sharaf, T. and Sadeghian, P., 2016. Fiber element model of sandwich panels with soft cores and composite skins in bending considering large shear deformations and localized skin wrinkling. Journal of Engineering Mechanics, 142(5), p.04016015.

[32] Triantafillou, T.C. and Gibson, L.J., 1990. Constitutive modeling of elastic-plastic open-cell foams. Journal of engineering mechanics, 116(12), pp.2772-2778.

[33] Elfordy, S., Lucas, F., Tancret, F., Scudeller, Y. and Goudet, L., 2008. Mechanical and thermal properties of lime and hemp concrete ("hempcrete") manufactured by a projection process. Construction and Building Materials, 22(10), pp.2116-2123.

[34] Betts, D., Sadeghian, P. and Fam, A., 2018. Experimental behavior and design-oriented analysis of sandwich beams with bio-based composite facings and foam cores. Journal of Composites for Construction, 22(4), p.04018020.

Table 1. Test matrix of beam specimens

Set #	Specimen group ID	Number of layers of jute fabric	Position of jute fabric (from bottom)	Number of identical specimens
1	L1-0.5H	1	H/2	3
2	L1-0.25H	1	H/4	3
3	L2-0.25H	2	H/4	3
Total	-	-	-	9

Note: H=height of beam specimen

Table 2. Summary compression test results

	Initial stiffness (kPa)	Yielding strength (kPa)	Densification stress (kPa)	Strain hardening stiffness (kPa)
Average value	3000	200	500	7000

Table 3. Summary of bending test results

Specimen group ID	Specimen #	Yielding		Failure		Energy(J)
		Load (N)	Displacement (mm)	Load (N)	Displacement (mm)	
L1-0.5H	1	114	3.0	122	5.1	0.4
	2	128	1.3	131	3.2	0.32
	3	122	2.6	127	4.4	0.4
	Average	**121**	**2.3**	**127**	**4.2**	**0.37**
	SD	**6**	**0.7**	**4**	**0.8**	**0.04**
L1-0.25H	1	294	7.4	337	13.6	3.4
	2	278	6.0	287	10.2	2
	3	209	5.0	232	8.6	2.2
	Average	**260**	**6.1**	**285**	**10.8**	**2.53**
	SD	**37**	**0.98**	**43**	**2.1**	**0.62**
L2-0.25H	1	263	10.3	284	23.9	5.8
	2	224	9.3	282	20.0	4.5
	3	268	4.9	281	19.3	4.9
	Average	**252**	**8.2**	**282**	**21.1**	**5.1**
	SD	**20**	**2.4**	**1.3**	**2.0**	**0.55**

SD: standard deviation

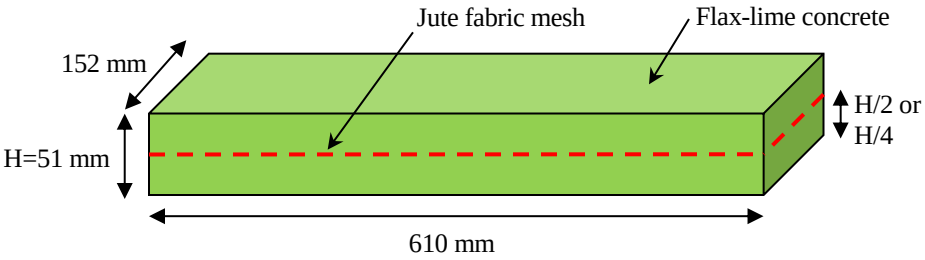

Figure 1. Geometry of beam specimens

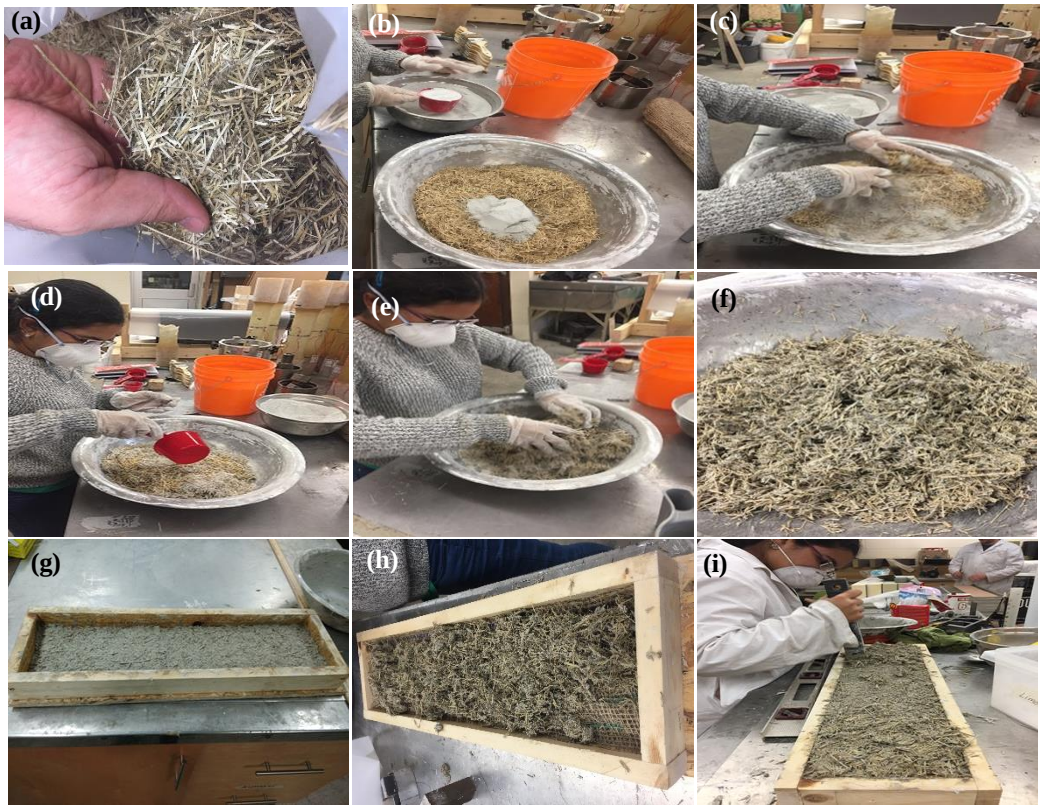

Figure 2. Specimen preparation: (a) flax shives; (b) adding binder to flax shives; (c) mixing binder with flax shives; (d) adding water to mix; (e) mixing water with flax and binder; (f) flax-lime mix ready to be used; (g) formwork filled and compacted to half; (h) jute fabric placed and next flax-lime layer cast; and (i) the last layer compacted.

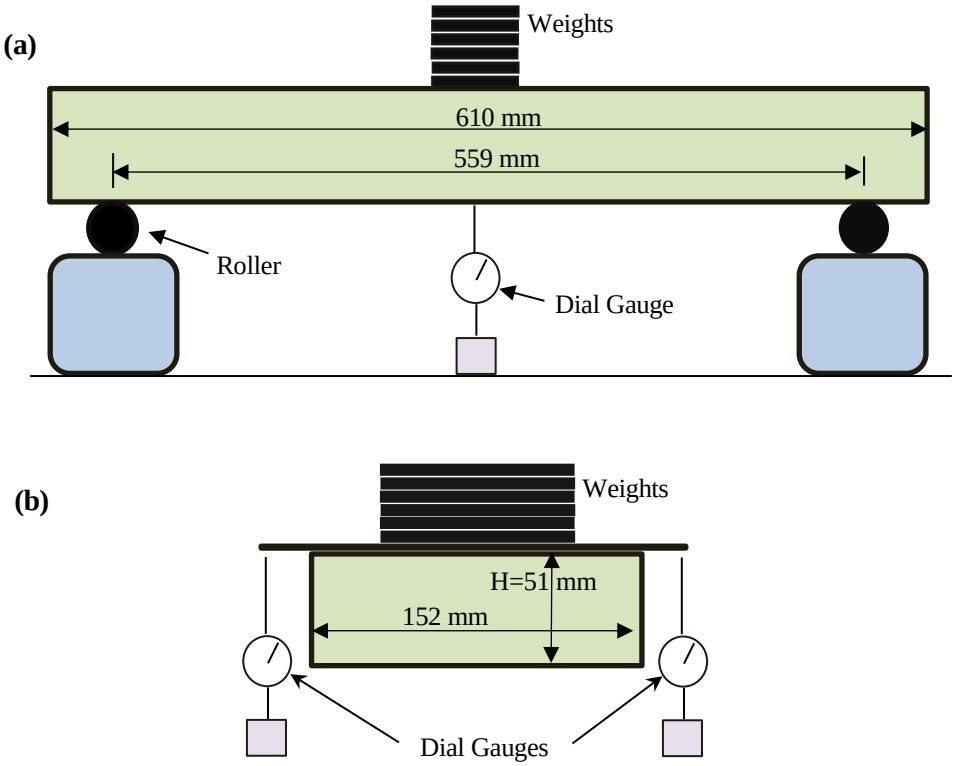

Figure 3. bending test setup schematics: (a) side view; and (b) cross-section (dimensions in mm)

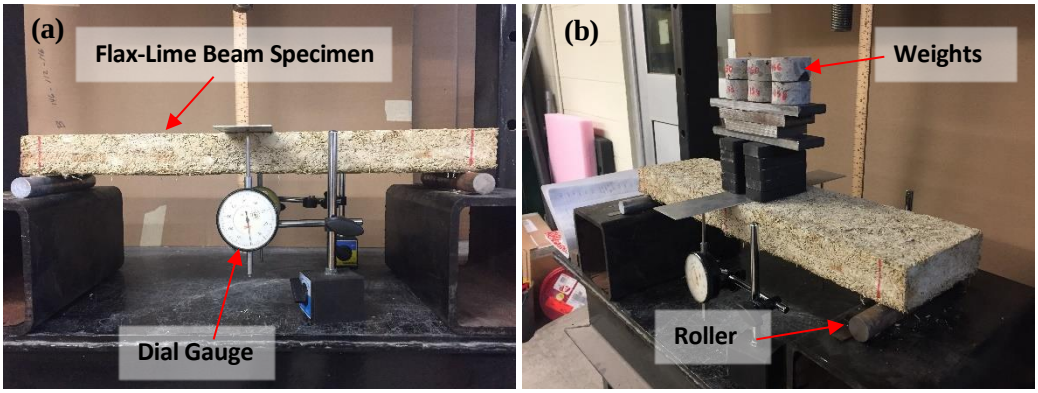

Figure 4. bending test setup photos: (a) before loading; and (b) loaded specimen.

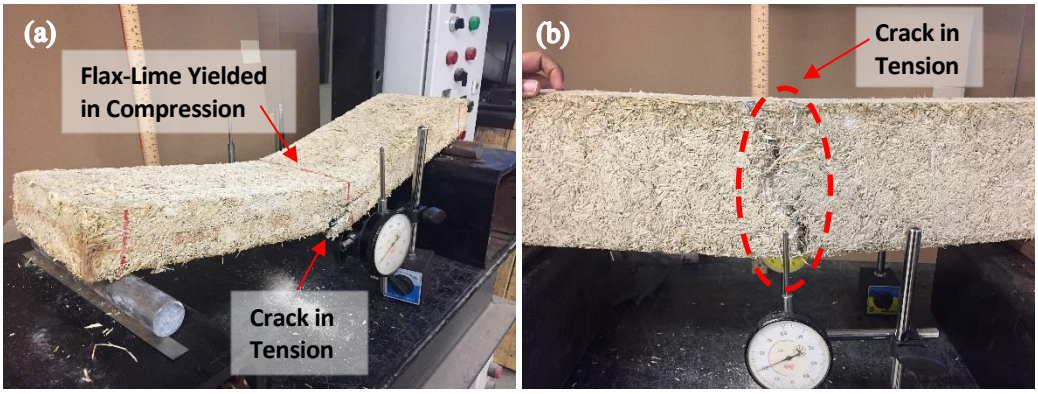

Figure 5. Typical bending failure mode: (a) side view; (b) bottom view.

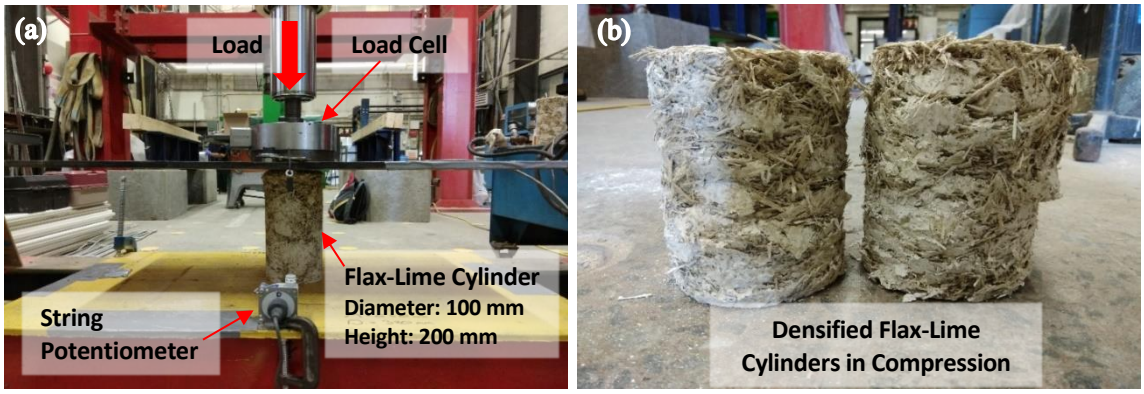

Figure 6. Compressive test of flax-lime concrete: (a) test setup; and (b) cylinder after the test.

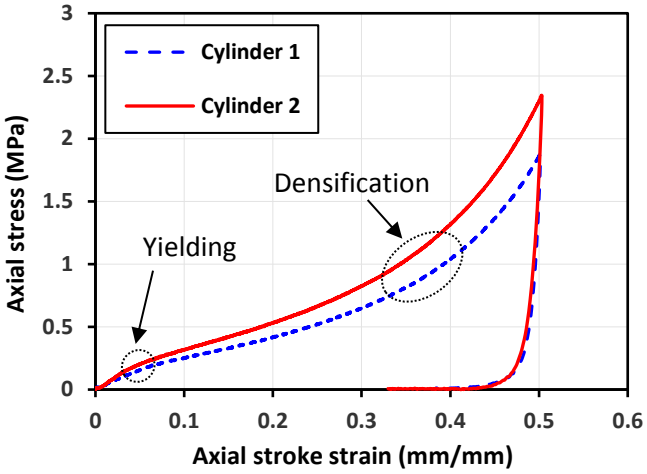

Figure 7. Compressive behavior of flax-lime concrete cylinders.

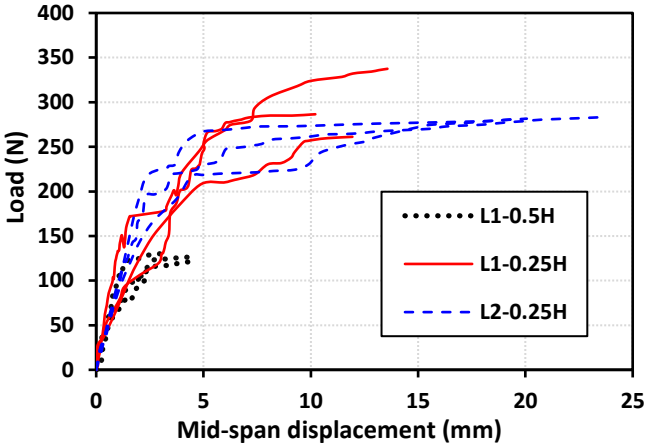

Figure 8. Load-deflection behavior of all beam specimens.

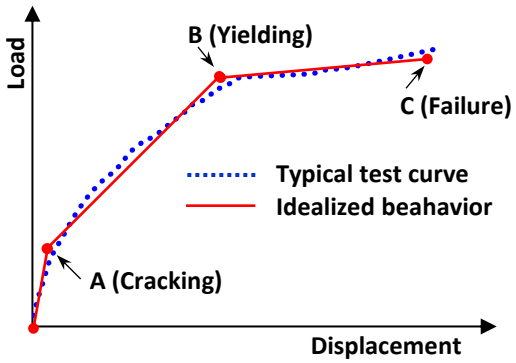

Figure 9. Idealized load-deflection behavior of flax-lime beam specimens reinforced with jute fabric.